On the motions and internal forces of a constrained floating body in linear waves

Wu, S.; Murray, J. J.; Winsor, F. N.

https://doi.org/10.4224/40003392

Institute Report (National Research Council of Canada. Institute for Marine Dynamics); no. IR-1993-08, 1993-07

National Research Council Canada
Conseil national de recherches Canada

Institute for Marine Dynamics
Institut de dynamique marine

Institute Report Rapport de l'Institut

IR-1993-08

ON THE MOTIONS AND INTERNAL FORCES OF A CONSTRAINED FLOATING BODY IN LINEAR WAVES

S. Wu, J. Murray and F. Winsor

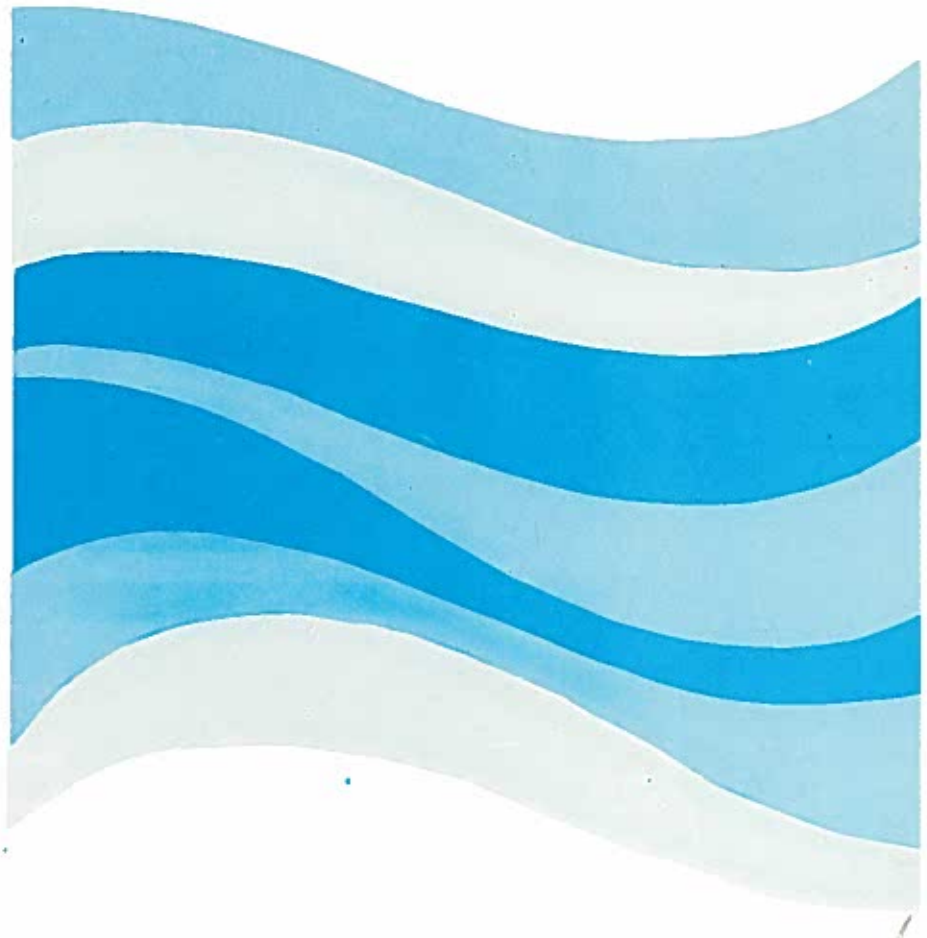

National Research Council Canada
Institute for Marine Dynamics

Conseil national de recherches Canada
Institut de dynamique marine

ON THE MOTIONS AND INTERNAL FORCES OF A CONSTRAINED FLOATING BODY IN LINEAR WAVES

IR-1993-08

S. Wu, J. Murray and F. Winsor

July 1993

DOCUMENTATION PAGE

REPORT NUMBER IR-1993-08	NRC REPORT NUMBER 33950	DATE July 1993
REPORT SECURITY CLASSIFICATION Unclassified		DISTRIBUTION Unlimited

TITLE

ON THE MOTIONS AND INTERNAL FORCES OF A CONSTRAINED FLOATING BODY IN LINEAR WAVES

AUTHOR(S)

S. Wu, J. Murray and F. Winsor

CORPORATE AUTHOR(S)/PERFORMING AGENCY(S)

Institute for Marine Dynamics
National Research Council Canada

PUBLICATION

To be submitted to Ocean Engineering Journal

SPONSORING AGENCY(S)

Institute for Marine Dynamics
National Research Council Canada

IMD PROJECT NUMBER 398 24	NRC FILE NUMBER -	

KEY WORDS:	PAGES	FIGS.	TABLES
linearized motions of a constrained floating body; wave induced internal forces	iv, 34, apps. A-F	8	-

SUMMARY:

The rigid body motions of floating offshore structures can be modelled as externally constrained floating bodies. This report centres on the calculation of the induced internal forces in these structures in regular waves as well as their motions. A floating body is assumed to consist two parts rigidly connected to each other. By assuming small amplitude body motions, detailed derivations are presented of the body motions, external and internal forces. Results from application of the formulations to the case of a semi-submersible platform are presented and compared with those from experiments. The formulation provides a useful tool for full-scale computations and model test design of several types of floating offshore platforms.

ADDRESS: National Research Council
Institute for Marine Dynamics
P. O. Box 12093, Station 'A'
St. John's, NF
A1B 3T5

Table of Contents

List of Figures

ON THE MOTIONS AND INTERNAL FORCES OF A CONSTRAINED FLOATING BODY IN LINEAR WAVES

SUMMARY

The rigid body motions of floating offshore structures can be modelled as externally constrainted floating bodies. This report centres on the calculation of the induced internal forces in these structures in regular waves as well as their motions. A floating body is assumed to consist two parts rigidly connected to each other. By assuming small amplitude body motions, detailed derivations are presented of the body motions, external and internal forces. Results from application of the formulations to the case of a semi-submersible platform are presented and compared with those from experiments. The formulation provides a useful tool for full-scale computations and model test design of several types of floating offshore platforms.

1.0 INTRODUCTION

Unlike seagoing ships, floating offshore structures are usually positioned at a given location at sea. Typical examples are semi-submersible platforms, TLPs, and moored tanker based floating offshore production systems. The positioning mechanism used on these structures may vary widely, but there is one thing in common, i.e., the motions of these structures at sea are externally constrained by the positioning mechanism.

The motions of a ship in waves as a rigid and freely floating body are among the most widely studied areas in ship hydrodynamics. The most frequently used approach is to assume small amplitude motions and considerable simplifications are then made to derive the linearized equations of motion. A number of publications can be referred to on this[1-3]. The formal derivation of the linearized equations of motion of a constrained floating body can also be found in a number of publications[4-6]. The linearization is achieved by perturbation in terms of the wave slope, kA, where k is the wave number and A is the amplitude. The hydrodynamic computations are usually done numerically by a three dimensional source distribution technique (or surface panel method)[7]. Comparatively speaking, studies on the induced internal loads are limited, mostly to the types of structures such as SWATH (small water-plane area twin hull) ships and other catamaran forms for which the induced internal loads are of prominent concern[8].

In what follows, a detailed formulation of the linearized motion equations and internal forces for a constrained floating body in regular waves is presented. In this, the body was divided into two parts without losing generality. The external forces and motions of each part were considered separately in a common reference frame and then combined to arrive at the motion equations of the whole body. Both the external and internal forces were decomposed into a constant component and a linearized motion dependent component. Having obtained the whole body motions, the internal forces between the two body parts were derived by considering the motions of one of the body parts only. This systematic approach provides great expedience in calculating the internal forces.

Application was then made of the formulations to the case of the motions of the semi-submersible, Glomar Arctic III. Model tests on the semi-submersible have been done at IMD[9] in which the motions of the semi-submersible in regular waves and the induced internal forces were measured. Correlation results between the measured motions and forces from model tests and those of the present numerical predictions are presented.

The present formulations are applicable directly to a wide range of floating offshore structures in waves, freely floating or constrained. The program will also be useful for model testing of these structures in the future. To facilitate use of the computer program, an auxiliary computer program is also written to compute the hydrostatic characteristics of these structures as documented in Appendix D. In it, these structures are regarded as consisting two basic mass elements: columns (a distributed mass model) and concentrated masses (a lumped mass model). While hydrostatic calculation can be done directly with concentrated masses, columns are divided into thin strips and integration is then carried out along the column length.

2.0 LINEARIZED EQUATIONS OF MOTION

2.1 The Dual Coordinate Systems

For convenience of derivation, two sets of coordinate systems are used. The motion of the fluid is more easily described in an inertial system fixed in space, whereas the geometrical configuration of the body in motion is more easily described in a system fixed in the body.

Referring to Figure 1, let the inertial coordinate system be $oxyz$ with oz opposing the direction of gravity and oxy lying parallel with the undisturbed free surface. Let $o'x'y'z'$ be fixed in the body. For simplicity, it is assumed that the three axes of $o'x'y'z'$ being parallel with, and pointing in the same direction as, those of the $oxyz$ system when the body is in the static equilibrium position. $\vec{P}$ symbolizes presence of external constraints. Denote $\vec{r}$ as the position vector of an arbitrary point on the body as viewed in the $oxyz$ system. The distance vector from o' to this point is denoted as $\vec{R}$. When viewed in the $o'x'y'z'$ system, this point has a position vector of

Figure 1 A constrained floating body and the dual coordinate systems ($\vec{P}$ represents external constraints).

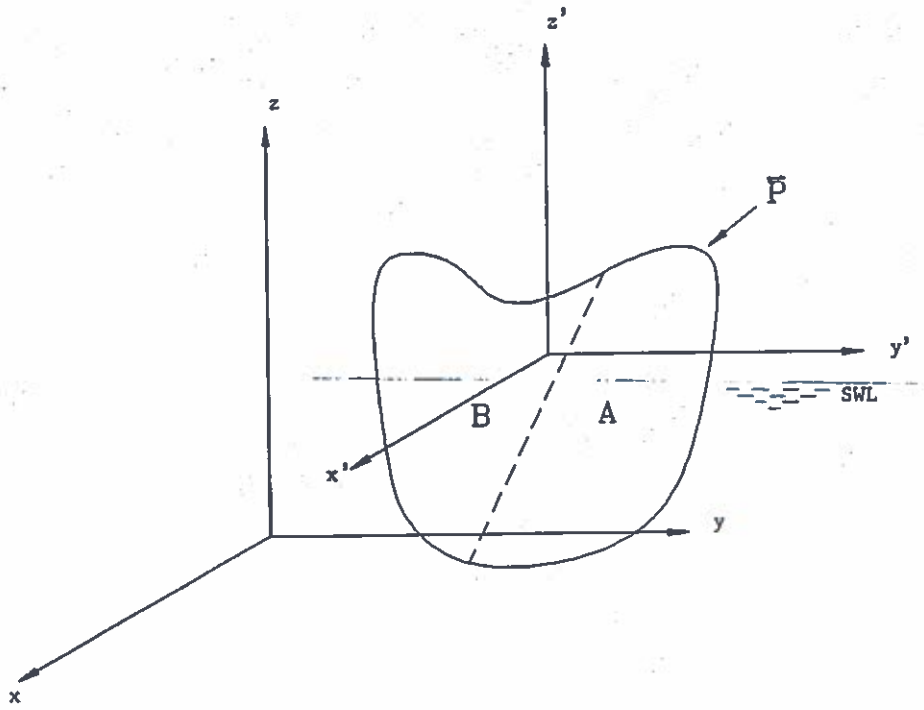

$\vec{r'}$. In addition, the position vector of o' in the $oxyz$ system is denoted as $\vec{r}_0$.

The rigid body motions of a constrained floating body as shown in Figure 1 can be described in terms of the six-degrees-of-freedom motion of the body at point o' on the body. Let

$$\vec{q} = (q_x, q_y, q_z) = (q_1, q_2, q_3) \tag{1}$$

$$\vec{\alpha} = (\alpha_x, \alpha_y, \alpha_z) = (q_4, q_5, q_6) \tag{2}$$

be the translational and angular displacement vector of the body at o' in the $oxyz$ system respectively with

$$\{q\} = \{q_1, ..., q_6\}^T \tag{3}$$

denoting the total displacement vector. The components represent surge, sway, heave, roll, pitch and yaw of the six-degrees-of-freedom motions of the body respectively and correspond to indices $j = 1, 2, ..., 6$. The superscript T denotes transpose of a matrix. In what follows, a similar indicial notation such that $\vec{r} = (x, y, z) = (r_1, r_2, r_3) = (x_1, x_2, x_3)$ is used interchangeably without being mentioned explicitly. The above

indicial notations are very useful as will become clear later.

Assuming that the motions are small then the two coordinate systems are related to each other by

$$\vec{r} = \vec{r}_o + \vec{R} = \vec{\bar{r}}_o + \vec{q} + \vec{r'} + \vec{\alpha} \times \vec{r'} \tag{4}$$

where overline is placed on top of a vector in the $oxyz$ system to represent the corresponding vector when the body is at its undisturbed position. The position vector of the body CG, $\vec{r}_G$ can now be expressed as

$$\vec{r}_G = \vec{r}_o + \vec{R}_G \tag{5}$$

where $\vec{R}_G$ represents the directional distance from point o' to the body CG in the $oxyz$ system.

It is noted that the rigid body motions can be described with respect to other reference points. In some literature, this reference point is taken to be the origin of the inertial coordinate system. In some other cases, the centres of rotation and gravity of the body have been used. Use of the origin of the $o'x'y'z'$ system as the reference point results in a mass matrix that is most sparse when points o and o' coincide at the undisturbed position of the body, but choice of the reference point is often made as a matter of convenience. The motion equations with respect to any other reference point can be obtained in a similar manner.

2.2 Conservation of Momentum

The equations of motion of the floating body in Figure 1 can be derived by considering conservation of the linear and angular momentum. For the purpose of computing the internal forces, the floating body may be decomposed into a number of rigidly connected parts. At present, it is divided into two parts without losing generality, namely, parts A and B as shown also in Figure 1. Their mass centres in the inertial coordinate system are $\vec{r}_G^A$ and $\vec{r}_G^B$ respectively. In the following derivation, superscripts A and B are used to denote quantities related to body part A and B respectively.

The two conservation of momentum equations can be expressed as follows

$$\vec{F} = \frac{d}{dt}\int_{V^A+V^B} \rho \vec{U} dV \tag{6}$$

$$\vec{M} = \frac{d}{dt}\int_{V^A+V^B} \rho \vec{r} \times \vec{U} dV \tag{7}$$

In the equations ρ is the density of the body mass and V^B means integration over the body volume of part B. $\vec{U}$ is the velocity vector at point $\vec{r}$ of the body. According to equation (4), it can be written in terms of the velocity at point o' of the body as

$$\vec{U} = \dot{\vec{q}} + \dot{\vec{\alpha}} \times \vec{R} \tag{8}$$

where the dots represent differentiation with respect to time. Substitution of equation (8) into equations (6) and (7) and the subsequent expansions are done in Appendix A.

Let $\{F\} = \{F_1, ..., F_6\}^T$ be the extended force vector corresponding to equation (3) with $\{F_1, F_2, F_3\} = \{F_x, F_y, F_z\}$ and $\{F_4, F_5, F_6\} = \{M_x, M_y, M_z\}$. The equations defining the conservation of momentum can be rewritten, according to equation (A.12), as

$$\{F\} = [M]\{\ddot{q}\} \tag{9}$$

where $[M] = [M]^A + [M]^B$ is the total mass matrix equalling the sum of that for part A and B and is given by

$$[M] = \begin{bmatrix} m & 0 & 0 & 0 & mz'_G & -my'_G \\ 0 & m & 0 & -mz'_G & 0 & mx'_G \\ 0 & 0 & m & my'_G & -mx'_G & 0 \\ 0 & -m\bar{z}_G & m\bar{y}_G & I_{11}+J_{11} & I_{12}+J_{12} & I_{13}+J_{13} \\ m\bar{z}_G & 0 & -m\bar{x}_G & I_{21}+J_{21} & I_{22}+J_{22} & I_{23}+J_{23} \\ m\bar{x}_G & -m\bar{y}_G & 0 & I_{31}+J_{31} & I_{32}+J_{32} & I_{33}+J_{33} \end{bmatrix} \tag{10}$$

In the equation $m = m^A + m^B$ is the total mass of the body; $I_{jk} = I^A_{jk} + I^B_{jk}$ are the second moments of inertia of the total body mass with respect to the body fixed coordinate system as defined in equation (A.10). $J_{jk} = J^A_{jk} + J^B_{jk}$ are defined similarly to I_{jk} in equation (A.11). It is noted that when $\vec{\bar{r}}_o = 0$, $J_{jk} = J^A_{jk} + J^B_{jk} = 0$ holds. and the mass matrix is symmetric. $J_{jk} = 0$ also holds when $\vec{r'}_G = 0$, i.e. when the origin of the body fixed coordinate system is at the body CG.

Next the force vector $\{F\}$ needs to be calculated. The total forces and their overturning moments about $\vec{r} = 0$ are written in general as

$$\vec{F} = -\int_{S^A+S^B} p\vec{n}dS - \int_{V^A+V^B} \rho g\vec{k}dV + \vec{D} \tag{11}$$

$$\vec{M} = -\int_{S^A+S^B} p\vec{r}\times\vec{n}dS - \int_{V^A+V^B} \rho g\vec{r}\times\vec{k}dV + \vec{E} \tag{12}$$

In the above equations $\vec{n}$ is the unit outward normal vector to the body surface. $\vec{k}$ is the unit vector in the z-axis direction. The surface integrals represent contribution of the pressure force over the surface of the body. It mainly comes from the hydrodynamic pressure on the submerged part of the body. Perturbation of the hydrostatic pressure due to the body motions will give rise to a restoring force component whereas the dynamic part can be further divided into two components. The first one is the effect of motion of the body in otherwise still fluid and is usually expressed in terms of an added hydrodynamic mass and a damping matrices. The second is the combined effect of the fluid motion in the absence of the body and diffraction of the fluid by the body when it is fixed.

The volume integrals represents contributions from the the gravitational force of the body mass. $\vec{D}$ and $\vec{E}$ are the external constraining forces and their moments about $\vec{r} = 0$ respectively. They are dealt with in Section 3 below.

2.3 Velocity Potential and Hydrodynamic Pressure

Without introduction to the background, a velocity potential can be defined to describe the field of fluid motion in the presence of a floating body. The assumption of small amplitude motions enables the potential to be decomposed as follows

$$\phi = Re\left\{\left[(\varphi_0+\varphi_7)+\sum_{j=1}^{6} Q_j\varphi_j\right]e^{i\omega t}\right\} \tag{13}$$

where Re means the real part of the complex formula. i is the complex unit. ϕ_0 and ϕ_7 are the amplitude of the incident and diffraction velocity potential respectively. The remainder are the radiation potentials due to the six-degree-of-freedom motions of the body. Q_j $(j = 1,2,...6)$ are the complex motion amplitudes defined from equation (3) as

$$\{q\} = Re\left\{\{Q\}e^{i\omega t}\right\} \tag{14}$$

This assumes that any transient motions have disappeared and the body is in a steady state of oscillation.

The above potentials satisfy the governing Laplace equation and other relevant boundary conditions. Computation of the velocity potentials is known as the wave diffraction and radiation problem. A brief statement of the problem is presented in Appendix C.

The velocity potentials, once obtained, are used to compute the fluid pressure according to the linearized Bernoulli's equation as

$$\begin{aligned} p &= -\rho_w g(z-h) - \rho_w \frac{\partial \phi}{\partial t} \\ &= -\rho_w g(z-h) - \rho_w Re\left\{\left[(\varphi_0+\varphi_7) + \sum_{j=1}^{6} Q_j \varphi_j\right] i\omega e^{i\omega t}\right\} \end{aligned} \tag{15}$$

where ρ_w is the density of the fluid and $z = h$ defines the height of the mean water level. The terms inside the curly bracket represent the dynamic pressure, whereas the first term in equation (15) is due to changes in the hydrostatic pressure component. Substitution of this equation into equations (11) and (12) yields the forces. Appendix B details the integration of the hydrostatic pressure force over the instantaneous submerged surface of the body. In Appendix C, the hydrodynamic pressure forces are computed. According to the appendices, the total force can be rewritten in matrix notation as

$$\{F\} = -[c]\{q\} + \{G\} + \{D\} + Re\left\{\{F^e\}e^{i\omega t}\right\} - \left[-\omega^2[a] + i\omega[b]\right]\{Q\}e^{i\omega t} \tag{16}$$

In the above equation $[c]$ is known as the restoring stiffness matrix and is given, according to equation (B.19), by

$$[c] = [c]^A + [c]^B \tag{17}$$

The $\{G\}$ vector contains the static terms related to the body without external constraints. It is written according to equation (B.18) as

$$\{G\} = \{G\}^A + \{G\}^B \tag{18}$$

$\{D\}$ combines $\vec{D}$ and $\vec{E}$ in equations (11) and (12). As is shown in Section 3, it can be written in the following form

$$\{D\} = \{D^{(0)}\} + \{D^{(1)}\} \tag{19}$$

with

$$\{D^{(0)}\} = \{D^{(0)}\}^A + \{D^{(0)}\}^B$$

being the static component when the body is in its undisturbed position, and

$$\{D^{(1)}\} = \{D^{(1)}\}^A + \{D^{(1)}\}^B = [c_h]\{q\}$$

being the motion dependent component. By equating equation (16) with equation (9) and rearranging terms, the hydrostatic and dynamic equilibrium equations are obtained as follows.

$$\{G\} + \{D^{(0)}\} = 0 \tag{20}$$

$$[M + a]\{\ddot{q}\} + [b]\{\dot{q}\} + [c - c_h]\{q\} = \{F^e\}e^{i\omega t} \tag{21}$$

in which $Re\{\}$ is dropped, but is implied from now on. Equation (20) yields the sufficient (but not necessary!) static stability condition, which can be easily verified for a free floating body. That is, $mg = \rho g \nabla$, which is the Archimedes' Principle, and $x'_b = x'_G$ and $y'_b = y'_G$, which means that the centre of buoyancy lies on the vertical axis through the body CG.

All the terms except $[c_h]$ are known to the case of a freely floating body. For a externally constrained floating body, $\{D\}$ is treated in Section 3. In this case, equation (20) yields six static equilibrium equations, from which the static components of the unknown constraining forces and moments involved in $[c_h]$ of equation (21) above can be computed.

To improve the numerical predictions, especially in the frequency range in which resonant responses occur, viscous effect may be included. The viscous effect is estimated according to a linearized form of Morison's equation[10]. It gives rise to two terms, namely, drag exciting force and viscous damping. More details are presented in Appendix E.

3.0 EXTERNAL CONSTRAINING FORCES

Take for example a constraining force, $\vec{P}$, that is applied to the body at point $\vec{r}_P$ on the body ($\vec{r'}_P$ with respect to the body fixed coordinate system). In terms of

the rigid-body motions of the body, the force is equivalent to it being applied at point $\vec{r} = 0$ plus an overturning moment about $\vec{r} = 0$, denoted as $\vec{M}_P$. If it is assumed that $\vec{P}$ is linear in terms of the body motions, it can then be decomposed into a constant term and a linear term as

$$\vec{P} = \vec{P}^{(0)} + \vec{P}^{(1)} = \vec{P}^{(0)} + [T]\{q\} \tag{22}$$

where the first term is the constraining force when the body is at rest. $[T]$ is a 3×6 matrix containing the linear force coefficients. For the case of external constraining forces exerted by a linear elastic spring attached to the body, the matrix $[T]$ can be easily derived as presented in Appendix F.

By neglecting the nonlinear terms, $\vec{M}_P$ is given as

$$\begin{aligned} \vec{M}_P &= \vec{\bar{r}}_P \times \vec{P}^{(0)} \\ &+ \vec{\bar{r}}_P \times \vec{P}^{(1)} \\ &+ (\vec{q} + \vec{\alpha} \times \vec{r'}_P) \times \vec{P}^{(0)} \end{aligned} \tag{23}$$

The first term is constant and the remaining terms in the equation are of first order, which represent contributions from perturbation of the force and motions respectively. By defining a matrix [A] in terms of a vector $\vec{A} = (A_1, A_2, A_3)$ as

$$[\mathrm{A}] = \begin{bmatrix} 0 & -A_3 & A_2 \\ A_3 & 0 & -A_1 \\ -A_2 & A_1 & 0 \end{bmatrix}$$

force $\vec{P}$ and its moment can be written in more concise terms as

$$\begin{aligned} \{P\} &= \{\vec{P}, \vec{M}_P\}^T = \begin{bmatrix} [I] & 0 \\ [\bar{\mathrm{r}}_P] & 0 \end{bmatrix} \{\vec{P}^{(0)}, 0\}^T \\ &+ \begin{bmatrix} [T] \\ [-\mathrm{P}^{(0)}], [\mathrm{P}^{(0)}][\mathrm{r'}_P] + [\bar{\mathrm{r}}_P][T] \end{bmatrix} \{q\} \\ &= [T_P^{(0)}]\{\vec{P}^{(0)}, 0\}^T + [T_P^{(1)}]\{q\} \end{aligned} \tag{24}$$

where $[I]$ is the 3×3 identity matrix.

An external overturning moment, $\vec{N}$ can be decomposed into two components similar to equation (21) as

$$\vec{N} = \vec{N}^{(0)} + \vec{N}^{(1)} = \vec{N}^{(0)} + [T_N]\{q\} \tag{25}$$

It can then be combined into equation (24) directly. Now the external constraining force vector $\{D\}$ is the sum of all the external forces and moments (on body parts A and B, separately calculated and then added) and is decomposed in a similar manner

$$\begin{aligned} \{D\} &= \{D^{(0)}\} + \{D^{(1)}\} \\ &= \sum \left\{ \vec{P}^{(0)}, \vec{\bar{r}}_P \times \vec{P}^{(0)} + \vec{N}^{(0)} \right\}^T \\ &+ \sum \left[[T_P^{(1)}] + \begin{bmatrix} 0 \\ [T_N] \end{bmatrix} \right] \{q\} \end{aligned} \tag{26}$$

which, when compared with equation (19), gives

$$[c_h] = \sum \left[[T_P^{(1)}] + \begin{bmatrix} 0 \\ [T_N] \end{bmatrix} \right] \{q\}$$

4.0 COMPUTATION OF INTERNAL SPLITTING FORCES

To compute the internal forces, the total rigid-body motions have to be obtained first. To do this, simple notations are used and the motion equations (21) can be expressed as

$$\left[-\omega^2 (M + a) + i\omega b + (c - c_h) \right] \{Q\} = [K^e]\{Q\} = \{F^e\} \tag{27}$$

This equation leads to

$$\{Q\} = [K^e]^{-1}\{F^e\} \tag{28}$$

To calculate the internal splitting forces between part A and part B, isolate part B and replace the effect of part A on part B by an unknown force vector F_u (including the unknown moment components) applied at point $\vec{r}_u$. Let the unknown moment and force

$$\vec{M}_u = \vec{M}_u^{(0)} + \vec{M}_u^{(1)} \tag{29}$$

$$\vec{F}_u = \vec{F}_u^{(0)} + \vec{F}_u^{(1)} \tag{30}$$

Dropping the second order terms, the following are obtained

$$\{F_u^{(0)}\} = \{\vec{F}_u^{(0)}, \vec{M}_u^{(0)}\}^T \tag{31}$$

$$\{F_u^{(10)}\} = \{0, \vec{q} \times \vec{F}_u^{(0)} + (\vec{\alpha} \times \vec{r'}_u) \times \vec{F}_u^{(0)}\}^T = [T_u^{(10)}]\{Q\}e^{i\omega t} \tag{32}$$

$$\{F_u^{(01)}\} = \{\vec{F}_u^{(1)}, \vec{\bar{r}}_u + \times \vec{F}_u^{(1)} + \vec{M}_u^{(01)}\}^T = [T_u^{(01)}]\{F_u^{(01)}\}e^{i\omega t} \tag{33}$$

$\vec{M}_u^{(0)}$ and $\vec{F}_u^{(0)}$ are computed from the static equilibrium equations of body B, given now by

$$\{G\}^B + \{D^{(0)}\}^B + \{F_u^{(0)}\} = 0 \tag{34}$$

$\{F_u^{(0)}\}$ is therefore known. $\{F_u^{(10)}\}$ is also known. The only unknowns are $\vec{F}_u^{(1)}$ and $\vec{M}_u^{(1)}$ in $\{F_u^{(01)}\}$.

The equations of motion of part B can now be obtained similarly as

$$\left[-\omega^2(M^B + a^B) + i\omega b^B + (c^B - c_h^B)\right]\{Q\} = \{F^e\}^B + [T_u^{(01)}]\{F_u^{(01)}\} + [T_u^{(10)}]\{Q\} \tag{35}$$

The unknown force vector is then computed from

$$\{F_u^{(01)}\} = [T_u^{(01)}]^{-1}\left\{\left[-\omega^2(M^B + a^B) + i\omega b^B + (c^B - c_h^B - T_u^{(10)})\right]\{Q\} - \{F^e\}^B\right\} \tag{36}$$

5.0 MOTIONS OF A SEMI-SUBMERSIBLE MODEL

In the following, the formulations presented above are applied to the prediction of the motions of a semi-submersible and the induced internal forces in regular waves. Model test was done with a 1:36 scale model of a Glomar Arctic III semi-submersible at IMD. A sketch of the model is shown in Figure 2. In the model tests, the six-degrees-of-freedom motions and internal splitting forces (and moments) at the mid-deck level in regular waves were measured. Further details of the model tests are found in ref. [9]. This section presents the correlation study between the test results and those from present numerical prediction. In addition, the effect of varying some of the design parameters on the motions and internal forces are investigated. The test results used here are those under condition 6 (50ft draught, regular waves, beam seas) of ref. [9]. Maximum design loads at mid-deck elevation occur in beam seas. In the numerical computations, the mooring lines were modelled as simple massless springs. The spring stiffness was obtained from model test measurements.

Before going on detailed computations, it is useful to qualitatively analyse the experimental results on the body motions and internal forces as contained in ref. [9]. For this, the body can be regarded roughly as having two planes of symmetry. The

slender nature of the two half bodies in the longitudinal direction indicates high degree of directional dependence of the body motions. The body undergoes little yaw motion when the wave direction is in either plane of symmetry. It is only significant in the vicinity of quartering seas. In contrast, pitch and surge motions become more significant as the wave direction approaches the longitudinal plane of symmetry, whereas roll and sway motions decrease. Comparatively speaking, the heave motion is not as direction dependent. Nonetheless, a higher heave motion in head seas occurs than in other directional seas due to decoupling of heave and roll. Separation of the two half bodies generally means that there will exist a cancellation frequency (in the practical wave frequency range) in the sway motion in directional seas, the effect of which becomes more pronounced as the wave direction approaches beam seas. This cancellation frequency occurs in the neighbourhood of a 4:1 wave length/beam ratio, which means that the cancellation is relatively high. Similarly use of separated columns on each half body accounts for existence of a cancellation frequency in surge in head seas.

The slender nature of the two half bodies also means that the wave exciting forces and the induced internal forces are relatively small in head seas in general. The internal loads (shear/tensile force and bending/torsional moments) in beam seas are of primary concern. In the present case, the bending moment $M_{ux}^{(1)}$ and tensile (compressional) force $F_{uy}^{(1)}$, which are the two critical internal load components from the structural strength point of view, are also the largest. The vertical shear force $F_{uz}^{(1)}$ is higher in beam seas than in other directional seas which is in contrast with the vertical motion. The longitudinal (horizontal) shear force, $F_{ux}^{(1)}$, torsional moment $M_{uy}^{(1)}$ and bending moment $M_{uz}^{(1)}$ are practically zero in beam seas, but become dominant in quartering seas. Their combined effect may be significant, but their individual amplitudes are much less than those of $F_{uy}^{(1)}$ and $M_{ux}^{(1)}$ in beam seas. It is therefore concluded that from the structural design point of view, the transverse tensile force $F_{uy}^{(1)}$ and bending moment $M_{ux}^{(1)}$ are the critical internal loads at the mid-deck level.

5.1 Motions

In Figures 3 to 5, the measured and numerically predicted body motions in beam seas are compared. Very good agreement is obtained for the sway motion. The same can be said about the heave motion except in the resonant frequency range

(around $T = 20.5$ seconds). Addition of linearized viscous damping as calculated in Appendix E improved the numerical results in this frequency range, but the linearized equations of motion are not entirely valid in the vicinity of the resonant frequencies. All the nonlinear effects would have to be included.

The measured roll motion is lower than numerically predicted. This is thought to be attributable to the insufficient resolution of the optical tracking system arrangement used in the tests to measure the roll motion. The optical tracking system had a resolution of 0.5°. The roll motion amplitude, which decreases as the wave period increases, was about 1° at frequencies between 9 and 19.5s and dropped below 1° quickly at long wave periods.

5.2 Wave Induced Internal Forces

For the present model in beam seas, the longitudinal surge splitting force, the pitch moment (torque) and the yaw moment (transverse bending) of the internal splitting force vector are near zero. Comparisons on the the remaining three force components are presented only. The results are shown in Figures 6 to 8. Again very good agreement is obtained between the numerical and model test results for the internal heaving shear force, $F_{uz}^{(1)}$, and rolling overturning moment, $M_{ux}^{(1)}$. Relatively abrupt changes occurred in the computed rolling overturning moment in the vicinity of heave resonant frequency as expected. A similarly abrupt change was also found for the transverse swaying force, $F_{uy}^{(1)}$, at these frequencies. The agreement on the sway force at other frequencies is generally good. The relatively large discrepancies between the numerical and the measured results of the sway force at high frequencies is attributed to the numerical exciting force computation. A single node Gaussian quadrature was used on each panel, which is expected to be acceptable at low frequencies, but is inaccurate at high frequencies. For the present structure with a longitudinal centre plane of symmetry, it can be easily shown that the internal transverse sway force is the difference between the sway exciting forces on the two half bodies.

5.3 The Mooring Effect

Results obtained with and without the mooring lines showed that presence of the mooring lines only affected the sway motions in relatively low frequency range (wave periods above 15s). Also, the peak of the internal force and moment RAOs (response amplitude operator) occurred at relatively high frequencies. In the practical wave frequency range up to 18 seconds, the mooring line effect can be safely neglected. This is expected as in this frequency range, the bulk of the total resistance to the wave exciting forces is from the inertia force. It is only in the very low drift wave frequency range, in which the response is largely quasi-static, that the restoring force contribution from the mooring lines becomes important. An interesting discussion was given by Miller and Wilson[11] on the effect of moorings and relevant design criteria.

5.4 Effect of Body Mass Distribution

Additional numerical computations were done to investigate the effect of structural mass distribution on the overall motions and internal forces of the semi-submersible. This was done in two separate ways: one with a vertical shift of the body CG only and one with a transverse shift of the CGs of the two half bodies. The geometrical dimensions were kept unchanged.

In the case of a 10% (9ft in absolute terms) downward shift of the body CG, the roll RAO was decreased slightly. The heave and sway RAOs were even less affected above the heave resonant frequency. The internal sway force was unchanged as expected. It can be shown theoretically that the internal sway force at the mid-deck level in the longitudinal plane of symmetry is the difference between the external sway exciting forces on the two half bodies. However, reduction of about 10% (or 0.3MN/m) was found in the maximum value of the internal roll moment RAO, which occurred at a wave period of around 9 seconds. At other wave periods outside this peak RAO range (see Figure 8), the change was much less significant. Similar changes in the internal heaving force were found. From practical design point of view, these changes do not substantially affect safety factor level.

In the case of transverse shift of the CGs of the two half bodies, a 2.0m maximum shift (representing a change of about 10%) for both half bodies away from the

centre line was considered. This resulted in an increased roll mass moment of inertia, and consequently a reduced roll RAO, but the sway and heave RAOs were not practically affected. The internal roll moment RAO was more or less unchanged in the peak frequency range, but increased at lower frequencies with a maximum of about 5%. The same was found with the internal heaving force.

In practice, variation of the body CG is limited. It is therefore concluded that variation of the body CG does not affect the body motions and internal forces significantly.

6.0 CONCLUSIONS

Detailed formulation of the motions of an externally constrained floating body and the induced internal forces in regular waves has been presented. The formulation was based on the assumption of small amplitude body motions. It included detailed treatment of the external constraining forces and calculation of the internal forces in the body, and was done systematically by decomposing the body into several rigidly connected parts. Application of the formulation to the case of the moored semi-submersible, Glomar Arctic III, indicated very good agreement between the numerical results on body motions and internal forces and those from model tests. The present formulation is directly applicable to full-scale study and model testing of a wide range of floating offshore structures.

Numerical results for the semi-submersible obtained with and without the mooring lines indicated that the mooring effect on the body motions and internal forces were practically insignificant in the wave frequency range.

Examination of the effect body mass distribution showed that due to limited variation of body CG in real design, the body mass distribution does not affect the body motion and internal forces at the mid-deck level substantially in the wave frequency range.

This report was prepared while Shukai Wu was visiting the Institute for Marine Dynamics – NRC as a NSERC Visiting Fellow. Assistance from staff of the Computational

Hydrodynamics Laboratory in providing access to the WAMIT computer program is gratefully acknowledged.

7.0 REFERENCES

1 Stoker, J.J., *Water Waves*, Interscience, 1957.

2 Wehausen, J.V., "The motion of floating bodies", *Annual Review of Fluid Mechanics*, vol. 3, pp237-268, 1971.

3 Newman, N.J., *Marine Hydrodynamics*, the MIT Press, Cambridge, Mass., 1977.

4 John, F., "On the motions of floating bodies I", *Communications on Pure and Applied Mathematics*, vol. 2, pp13-57, 1949.

5 John, F., "On the motions of floating bodies II", *Communications on Pure and Applied Mathematics*, vol. 3, pp45-101, 1950.

6 Mei, C.C., *The Applied Dynamics of Ocean Surface Waves*, World Scientific, London, 1989 (2nd Printing).

7 Newman, J.N. and Sclavounos, P.D., "The computation of wave loads on large offshore structures", *BOSS'88, Proceedings of the International Conference on the Behaviour of Offshore Structures*, Trondheim, Norway, 1988, vol. 2, pp605-622.

8 Reilly, E.T., Shin, Y.S. and Kotte, E.H., "A prediction of structural load and response of a SWATH ship in waves", *Naval Engineers Journal*, May 1988, pp251-264.

9 Murray, J.J., and Wu, S., Winsor, F., "An investigation into the response of the Glomar Arctic III semi-submersible with sponsons", TR-1993-13, Institute for Marine Dynamics – NRC, 1993.

10 Chakrabarti, S.K., *Hydrodynamics of Offshore Structures*, Springer-Verlag, New York, 1987.

11 Miller, N.S. and Wilson, P.M., "The Design wave conditions for determining wave drift forces on moored ships and semi-submersibles", *BOSS'92*, pp265-279.

APPENDIX A DERIVATION OF THE MASS MATRIX

A1. Body Motions

In the dual coordinate systems defined in Section 2.1, the following relationships from equation (4) are repeated

$$\vec{r} = \vec{r}_o + \vec{R} \tag{A.1}$$
$$\vec{R} = \vec{r'} + \vec{\alpha} \times \vec{r'} \tag{A.2}$$
$$\vec{r}_o = \vec{\bar{r}}_o + \vec{q} \tag{A.3}$$
$$\dot{\vec{r}} = \vec{U} = \dot{\vec{q}} + \dot{\vec{\alpha}} \times \vec{R} \tag{A.4}$$

A2. Linear Momentum

Now the linear momentum of the body mass of part B is

$$\begin{aligned} \vec{L} = \int_{V^B} d\vec{L} &= \int_{V^B} \vec{U} dm \\ &= m^B \dot{\vec{q}} + \dot{\vec{\alpha}} \times \int_{V^B} \vec{R} dm \\ &= m^B \dot{\vec{q}} + m^B \dot{\vec{\alpha}} \times \vec{R}_G^B \end{aligned} \tag{A.5}$$

where $\vec{R}_G$ is the directional distance of the body CG from point o' and is given by

$$\vec{R}_G^B = \frac{1}{m^B} \int_{V^B} \vec{R} dm \tag{A.6}$$

Conservation of linear momentum of the body is then expressed as

$$\vec{F}^B = \dot{\vec{L}} = m^B \ddot{\vec{q}} + m^B \ddot{\vec{\alpha}} \times \vec{R}_G^B + m \dot{\vec{\alpha}} \times \left(\dot{\vec{\alpha}} \times \vec{R}_G^B \right) \tag{A.7}$$

A3. Angular Momentum

The angular momentum of the body about the origin of the inertial coordinate system, denoted as $\vec{\Omega}$, is written as

$$\begin{aligned} \vec{\Omega} &= \int_{V^B} \vec{r} \times d\vec{L} \\ &= \int_{V^B} \vec{r} \times \vec{U} dm \end{aligned} \tag{A.8}$$

Conservation of angular momentum is then expressed as

$$\vec{M}^B = \dot{\Omega} = m^B \ddot{\vec{r}}_G^B \times \ddot{\vec{q}} + \sum_{k=1}^{3} \sum_{j=1}^{3} (I_{kj}^B + J_{kj}^B) \ddot{\alpha}_j \vec{i}_k + 0(q^2) \tag{A.9}$$

In the equation, $\vec{i}_k = \mathrm{i}, \mathrm{j}, \mathrm{k}$ for $k = 1, 2, 3$ respectively; $0(q^2)$ indicates the sum of terms that are of at least second order with respect to $\{q\}$; I_{jk}^B and J_{jk}^B are given by

$$I_{jk}^B = \int_{V^B} \rho(\vec{r'} \cdot \vec{r'} \delta_{jk} - r'_k r'_j) dV \tag{A.10}$$

$$\begin{aligned} J_{jk}^B &= \int_{V^B} \rho(\vec{\bar{r}}_o \cdot \vec{r'} \delta_{jk} - \bar{r}_{ok} r'_j) dV \\ &= m^B [\vec{\bar{r}}_o \cdot \vec{r'}_G^B \delta_{jk} - \bar{r}_{ok} r'^B_{Gk} \end{aligned} \tag{A.11}$$

where δ_{jk} is the Kroenecker δ function; and $\vec{r'} = (x', y', z') = (r'_1, r'_2, r'_3)$. $j, k = 1, 2, 3$. J_{jk}^B is similar in form to I_{jk}^B.

A4. The Mass Matrix in the Linearized Equations of Motion

By neglecting all the second and higher order terms with respect to the body motions, $\{q\}$, The two conservation of momentum equations above are then combined in matrix form as follows.

$$[M]^B = \begin{bmatrix} m & 0 & 0 & 0 & mz'_G & -my'_G \\ 0 & m & 0 & -mz'_G & 0 & mx'_G \\ 0 & 0 & m & my'_G & -mx'_G & 0 \\ 0 & -m\bar{z}_G & m\bar{y}_G & J_{11}+I_{11} & J_{12}+I_{12} & J_{13}+I_{13} \\ m\bar{z}_G & 0 & -m\bar{x}_G & J_{21}+I_{21} & J_{22}+I_{22} & J_{23}+I_{23} \\ -m\bar{y}_G & m\bar{x}_G & 0 & J_{31}+I_{31} & J_{32}+I_{32} & J_{33}+I_{33} \end{bmatrix}^B \tag{A.12}$$

which are all zero if $\vec{\bar{r}}_o = 0$ is chosen, i.e. the inertial and body fixed coordinate systems coincide in the undisturbed position of the body.

APPENDIX B DERIVATION OF THE RESTORING STIFFNESS MATRIX

When equation (15) is substituted into equation (11), the first term is an integral of the form $\rho_w g \int_{S^A+S^B}(z-h)\{n\}dS$ which represents the force vector due to hydrostatic pressure over the submerged body surface. Carrying out the integration for part B and denoting also as $\vec{F}^B$ for simplicity

$$\begin{aligned}\frac{\vec{F}^B}{\rho_w g} &= \int_{S^B}\vec{n}(z-h)dS \\ &= \oint_{S^B}\vec{n}z dS - \int_{S_w^B}\vec{\mathrm{k}}(z-h)dS\end{aligned} \tag{B.1}$$

where S_w^B indicates the waterplane area of body part B. By virtue of Gauss' theorem

$$\oint_{S^B}\vec{n}f dS = \int_{V^B}\nabla f dS \tag{B.2}$$

in which ∇ represents the gradient of a scalar function. The surface integral over S_w^B is zero in equation (B.1). Therefore,

$$\frac{\vec{F}^B}{\rho_w g\vec{\mathrm{k}}} = \int_{V_0^B-\Delta V^B} dV \tag{B.3}$$

where V_0^B represents the mean submerged volume and ΔV^B represents the difference between the mean and the instantaneous volume of submergence of body part B.

$$dV = \Delta z dx'dy' = q_3 + (\vec{\alpha}\times\vec{r'})_3 dx'dy' = (q_3+\alpha_1 y' - \alpha_2 x')dx'dy' \tag{B.4}$$

$$\begin{aligned}\frac{\vec{F}^B}{\rho_w g\vec{\mathrm{k}}} &= \nabla^B - \int_{\Delta V^B} dV \\ &= \left[\nabla^B - (S_w q_3 + \alpha_1 S_2 - \alpha_2 S_1)\right]\end{aligned} \tag{B.5}$$

where ∇^B is the displacement of part B. The above equation can be written in matrix form for part B of the body as

$$\vec{F}^B = \rho_w g\vec{\mathrm{k}}\left\{\nabla - \begin{bmatrix}0&0&0&0&0&0\\0&0&0&0&0&0\\0&0&S_w&S_2&-S_1&0\end{bmatrix}\{q\}\right\}^B \tag{B.6}$$

where

$$S_j^B = \int_{S_w^B} x'_j dx'_1 dx'_2 \tag{B.7}$$

is the polar moment of the waterplane area of part B defined in terms of the body fixed coordinate system.

In a similar manner, the moment integration can be expanded as follows

$$\begin{aligned}\frac{\vec{M}^B}{\rho_w g} &= \int_{S^B} \vec{r}\times\vec{n}(z-h)dS \\ &= \oint_{S^B} \vec{r}\times\vec{n}(z-h)dS - \int_{S_w^B} \vec{r}\times\vec{n}(z-h)dS \\ &= -\int_{V^B} \nabla\times\vec{r}(z-h)dV - \int_{S_w^B} \vec{r}\times\vec{k}(z-h)dS \\ &= -\int_{V_0^B-\Delta V^B} (-y\vec{i}+x\vec{j})dV\end{aligned} \tag{B.8}$$

according to Gauss' theorem

$$\oint_{S^B} \vec{r}\times\vec{n}z dS = \int_V \nabla\times\vec{r}z dV \tag{B.9}$$

From equation (5) of Section 2.2

$$y = y_o + y' + q_2 + \alpha_3 x' - \alpha_1 z' \tag{B.10}$$

$$x = x_o + x' + q_1 + \alpha_2 z' - \alpha_3 y' \tag{B.11}$$

$$\int_{V_0^B} -y\vec{i}dV = -\vec{i}\nabla^B\left[y_o + y'_b + q_2 + \alpha_3 x'_b - \alpha_1 z'_b\right]^B \tag{B.12}$$

$$\begin{aligned}-\int_{\Delta V^B} -y\vec{i}dV &= \vec{i}\left[y_o(S_w q_3 + \alpha_1 S_2 - \alpha_2 S_1)\right. \\ &\quad \left.+(q_3 S_2 + \alpha_1 S_{22} - \alpha_2 S_{12})\right]^B\end{aligned} \tag{B.13}$$

$$\int_{V_0^B} x\vec{j}dV = \vec{j}\nabla^B\left[x_o + x'_b + q_1 + \alpha_2 z'_b - \alpha_3 y'_b\right]^B \tag{B.14}$$

$$\begin{aligned}-\int_{\Delta V^B} x\vec{j}dV &= -\vec{j}\left[x_o(S_w q_3 + \alpha_1 S_2 - \alpha_2 S_1)\right. \\ &\quad \left.+(q_3 S_1 + \alpha_1 S_{12} - \alpha_2 S_{11})\right]^B\end{aligned} \tag{B.15}$$

$$\begin{aligned}\frac{\vec{M}^B}{\rho_w g} &= -\Big\{-\vec{i}\left[\nabla(y_o + y'_b + q_2 + \alpha_3 x'_b - \alpha_1 z'_b)\right. \\ &\quad \left.-y_o(S_w q_3 + \alpha_1 S_2 - \alpha_2 S_1) - (q_3 S_2 + \alpha_1 S_{22} - \alpha_2 S_{12})\right] \\ &\quad +\vec{j}\left[\nabla(x_o + x'_b + q_1 + \alpha_2 z'_b - \alpha_3 y'_b)\right. \\ &\quad \left.-x_o(S_w q_3 + \alpha_1 S_2 - \alpha_2 S_1) - (q_3 S_1 + \alpha_1 S_{12} - \alpha_2 S_{11})\right]\Big\}^B\end{aligned} \tag{B.16}$$

$\vec{r'}^B_b$ represents the position vector of the centre of buoyancy of the submerged volume of part B in the body fixed coordinate system. S^B_{jk} is defined as

$$S^B_{jk} = \int_{S^B_w} x'_j x'_k dx'_1 dx'_2 \qquad k,j = 1,2,3$$

The second term in equation (12) of Section 2.2 represents the moment of the gravitational force and can be caculated for part B of the body as follows

$$\begin{aligned} -\int_{V^B} \rho g \vec{r} \times \vec{k} dV &= \rho g \int_{V^B} (-\vec{i}y + \vec{j}x) dV \\ &= -\vec{i} m^B g \left[y_o + y'^B_G + q_2 + \alpha_3 x'^B_G - \alpha_1 z'^B_G \right] \\ &+ \vec{j} m^B g \left[x_o + x'^B_G + q_1 + \alpha_2 z'^B_G - \alpha_3 y'^B_G \right] \end{aligned} \tag{B.17}$$

Combine the hydrostatic terms into $\{G\}$ to obtain, for body part B,

$$\{G\}^B = g\left\{0, 0, (\nabla^B \rho_w - m^B), (\nabla^B \rho_w \bar{y}^B_b - m^B \bar{y}^B_G), -(\nabla^B \rho_w \bar{x}^B_b - m^B \bar{x}^B_G), 0\right\}^T \tag{B.18}$$

where ∇^B now is the displaced volume of body part B when it is at its undisturbed position. The motion dependent terms in equations (B.6), (B.16) and (B.17) can be written in the form of $-[c]^B\{q\}$ in which $[c]^B$ is known as the restoring stiffness matrix and is given as

$$\frac{[c]^B}{\rho_w g} = \begin{bmatrix} 0 & 0 & 0 & 0 & 0 & 0 \\ 0 & 0 & 0 & 0 & 0 & 0 \\ 0 & 0 & S_w & S_2 & -S_1 & 0 \\ 0 & -\nabla + \frac{m^B}{\rho_w} & y_o S_w + S_2 & \nabla z'_b - \frac{m^B z'^B_G}{\rho_w} + S_{22} + S_2 y_o & -S_1 y_o - S_{12} & -\nabla x'_b + \frac{m^B x'^B_G}{\rho_w} \\ \nabla - \frac{m^B}{\rho_w} & 0 & -S_w x_o - S_1 & -S_2 x_0 - S_{12} & \nabla z'_b - \frac{m^B z'^B_G}{\rho_w} + S_{11} + S_1 x_o & -\nabla y'_b + \frac{m^B y'^B_G}{\rho_w} \\ 0 & 0 & 0 & 0 & 0 & 0 \end{bmatrix}^B \tag{B.19}$$

where $\vec{\bar{r}}^B_G = \vec{\bar{r}}_o + \vec{r'}^B_G$ is the position vector of the CG of body part B.

APPENDIX C STATEMENT OF THE RADIATION & DIFFRACTION PROBLEM

Denote $P = P(x, y, z)$ as the field point off the body surface (and $P(x, y, z) = p(x, y, z)$ on the body surface) and $q = (\xi, \zeta, \eta)$ as the source point on the body surface. The source potential at point $P(x, y, z)$ due to source distribution on the body surface (rigid) is

$$\phi(P) = \int_S \sigma(q) G(P, q) dS \tag{C.1}$$

The gradient of $\phi(P)$ at P in the direction of $\vec{n}_p$, when P outside the body surface is allowed to approach p on the body surface is then

$$\frac{\partial \phi(p)}{\partial n_p} = \lim_{P \to p; S_\epsilon \to 0} \int_{S_o + S_\epsilon} \sigma(q) \frac{\partial G(P, q)}{\partial n_p} dS = -2\pi\sigma(p) + \int_{S_o} \sigma(q) \frac{\partial G(p, q)}{\partial n_p} dS \tag{C.2}$$

where $S = S_o + S_\epsilon$ is divided with S_ϵ being the indented hemi-sphere at p. Upon imposing the body boundary conditions, the left-hand side of the equation is known. The equation is solved numerically to obtain the source density.

Let the total potential be

$$\phi = \varphi e^{k\omega t} = \sum_{j=0}^{7} \phi_j = \left[(\varphi_0 + \varphi_7) + \sum_{j=1}^{6} Q_j \varphi_j \right] e^{k\omega t} \tag{C.3}$$

where $j = 0, 1, ..., 7$ represents the incident, radiation and diffraction potentials respectively; $k = i$ or $-i$ may be used. Now the diffraction potential satisfies

$$\frac{\partial(\varphi_0 + \varphi_7)}{\partial n} = 0 \tag{C.4}$$

which leads directly to

$$\frac{\partial \varphi_7}{\partial n} = -\frac{\partial \varphi_0}{\partial n} \tag{C.5}$$

Let

$$n_j = n_j$$

for $j = 1, 2, 3$ and

$$n_j = \left(\vec{r'} \times \vec{n} \right)_{j-3}$$

for $j = 4, 5, 6$. Applying the flow tangency condition on the body surface leads to

$$\sum_{j=1}^{6} Q_j \frac{\partial \varphi_j}{\partial n} e^{k\omega t} = \vec{U} \cdot \vec{n} = k\omega \left[\vec{Q} \cdot \vec{n} + (\vec{r'} \times \vec{n}) \cdot \vec{\Omega} \right] e^{k\omega t}$$

This gives

$$\frac{\partial \varphi_j}{\partial n} = k\omega n_j \tag{C.6}$$

for $j = 1, 2, ..., 6$. Equations (C.5) and (C.6) are then substituted into equation (C.2), which is solved numerically for the source density function σ. Now the total potential amplitude can be obtained according to equation (C.1) on the body surface.

The dynamic pressure is then

$$\begin{aligned} p = -\rho_w \frac{\partial \phi}{\partial t} &= -k\rho_w \omega \varphi e^{k\omega t} \qquad (C.7) \\ &= -k\rho_w \omega(\varphi_0 + \varphi_7)e^{k\omega t} - k\rho_w \omega \sum_{j=1}^{6} Q_j \varphi_j e^{k\omega t} \end{aligned}$$

The pressure force and moment about a given point in the global coordinate system with position vector $\vec{r}_m$ are then computed as

$$\vec{F} = -\int_S p\vec{n}dS = \int_S \left\{ k\rho_w \omega(\varphi_0 + \varphi_7) - \left[-k\rho_w \omega \sum_{j=1}^{6} Q_j \varphi_j \right] \right\} \vec{n} e^{k\omega t} dS \tag{C.8}$$

$$\begin{aligned} \vec{M} &= -\int_S p(\vec{r} - \vec{r}_m) \times \vec{n} dS \qquad (C.9) \\ &= \int_S \left\{ k\rho_w \omega(\varphi_0 + \varphi_7) - \left[-k\rho_w \omega \sum_{j=1}^{6} Q_j \varphi_j \right] \right\} (\vec{r} - \vec{r}_m) \times \vec{n} e^{k\omega t} dS \end{aligned}$$

Define $m_j = n_j$ for $j = 1, 2, 3$ and $m_j = [(\vec{r} - \vec{r}_m) \times \vec{n}]_{j-3}$ for $j = 4, 5, 6$. This enables the above equations to be simply written as

$$F_\beta = \int_S \left\{ k\rho_w \omega(\varphi_0 + \varphi_7) - \left[-k\rho_w \omega \sum_{j=1}^{6} Q_j \varphi_j \right] \right\} m_\beta e^{k\omega t} dS \tag{C.10}$$

for $\beta = 1, 2, ..., 6$ representing the dynamic pressure forces and their moments about the given point. F_β is usually further decomposed into a wave exciting force (moment) component due to the combined incident and diffracted velocity potentials and a component directly proportional to the motion amplitudes as

$$F_\beta = \left[F_\beta^e - \sum_{j=1}^{6} F_{\beta j}^r Q_j \right] e^{k\omega t}$$

with

$$F_\beta^e = k\rho_w \omega \int_S (\varphi_0 + \varphi_7) m_\beta dS \tag{C.11}$$

$$F_{\beta j}^r = -k\rho_w \omega \int_S m_\beta \varphi_j dS \tag{C.12}$$

The part due to the incident and diffracted potentials in the first equation is referred to as the Froude-Kryvlov Force and diffraction force respectively, whereas the second equation is further decomposed into the following form

$$F^r_{\beta j} = k^2\omega^2 a_{\beta j} + k\omega b_{\beta j} \tag{C.13}$$

where $a_{\beta j}$ and $b_{\beta j}$, both real are known as the added mass and damping respectively.

APPENDIX D A HYDROSTATICS COMPUTER PROGRAM

To calculate the motion response ans internal forces of floating offshore structures such as TLPs and semi-submersibles, it is necessary to obtain the hydrostatic characteristics for part and/or the whole of the structure. Most offshore structures consists of column members. The cross-sectional shape of these column member may be circular, rectangular (or square), elliptic or triangular. In addition, the cross section may be hollow or solid. For the present purpose, it is sufficient to divide the structure into column members and lumped masses. Here "column" is used broadly as a mathematical model to represent any structural components having a mass distribution that cannot be regarded as lumped masses.

The definitions are well known. The algorithm is based on dividing each column into a number of segments (thin strips) and summation of the characteristics is carried out over all the segments to arrive at the total for the column.

In the case of a hollow column filled with ballasting material inside, for example, sea water, the column may be decomposed into two concentric columns: the hollow column itself and a solid column of the ballasting material. From the point of view of computing the hydrostatics of the structure, it is sufficient to consider the hydro-statics of a single column. Those for the whole structure is the sum of all the individual columns.

D1. Specification of a Column

A column is completely defined by the position vectors of of the column axis at its two ends, $\vec{r}_1$ and $\vec{r}_2$, the cross-sectional shape and orientation. The cross-sectional shape are defined in terms of four parameters in general, s_n for $n = 1, 2, 3$ and 4. They are as follows.

For a circular section:
$s_1 = R$ is the radius;
$s_4 = t$ is the shell thickness for a hollow section; and
for a solid cross section $s_4 \geq s_1$ is set.

For a rectangular section:
$s_1 = a$ is the length of the cross section;
$s_2 = b$ is the breadth of the cross section;
$s_4 = t$ is the shell thickness for a hollow section; and
for a solid cross section $s_4 \geq s_1$ is set.

For an elliptic section:
$s_1 = a$ is half the major axis of the cross section;
$s_2 = b$ is half the minor axis of the cross section;
$s_4 = t$ is the shell thickness for a hollow section; and
for a solid cross section $s_4 \geq s_1$ is set.

For a triangular section:
$s_1 = a$ is the bottom length of the cross section;
$s_2 = b$ is the isolateral of the cross section;
$s_4 = t$ is the shell thickness for a hollow section; and
for a solid cross section $s_4 \geq max(s_1, s_2)$ is set.

The orientation of the cross section can be defined in terms of the directions of its three principal axes. If the column axis passes through the centroid of the cross-section, then a unit normal of the cross section can be chosen as

$$\vec{e}_z = \frac{\vec{r}_2 - \vec{r}_1}{|\vec{r}_2 - \vec{r}_1|} \tag{D.1}$$

In this case, only one more principal axis of the cross section needs to be specified. Let $\vec{e}_x$ be the the unit vector along this principal axis. For a column of circular section, $\vec{e}_x$ is quite arbitrary. For convenience, $\vec{e}_x$ is defined as

$$\begin{aligned} \vec{e}_x &= \vec{\mathrm{k}} \times \vec{e}_z \quad \text{if } \vec{\mathrm{k}} \not\parallel \vec{e}_z \\ \vec{e}_x &= \vec{\mathrm{i}} \qquad\quad \text{if } \vec{\mathrm{k}} \parallel \vec{e}_z \end{aligned} \tag{D.2}$$

For other cross-sectional shapes, $\vec{e}_x$ is assumed to be as follows: $\vec{e}_x$ is parallel with the longer lateral of the rectangular section, the major axis of the elliptic section, and the bottom of the triangular section. In the latter cases, $\vec{e}_x$ needs to be specified. The unit vector along the third principal axis of the cross section is then

$$\vec{e}_y = \vec{e}_z \times \vec{e}_x \tag{D.3}$$

D2. Cross-Sectional Characteristics

These include the area and the second moments of inertia about the principal axes of the cross section. By definition, the polar moments of inertia of the cross section are identically zero. For convenience, let σ_1 and σ_2 be the area enclosed by the outside and inside peripherals of a hollow cross section respectively. For a solid cross section, $\sigma_2 = 0$. The solid area of the cross section is therefore

$$\sigma = \sigma_1 - \sigma_2 \tag{D.4}$$

The second moments of inertia of the solid area of the cross section are computed as follows.

$$I_{xx} = I_{yy} = \sigma_1 \frac{s_1^2}{4} - \sigma_2 \frac{(s_1 - s_4)^2}{4} \tag{D.5}$$

for circular section.

$$I_{xx} = \sigma_1 \frac{s_1^2}{12} - \sigma_2 \frac{(s_1 - 2s_4)^2}{12} \tag{D.6}$$

$$I_{yy} = \sigma_1 \frac{s_2^2}{12} - \sigma_2 \frac{(s_2 - 2s_4)^2}{12} \tag{D.7}$$

for rectangular section.

$$I_{xx} = \sigma_1 s_2^2/4 - \sigma_2 (s_2 - s_4)^2/4 \tag{D.8}$$

$$I_{yy} = \sigma_1 s_1^2/4 - \sigma_2 (s_1 - s_4)^2/4 \tag{D.9}$$

approximately for elliptic section.

$$I_{xx} = \sigma_1 s_1^2/24 - \sigma_2 \left(s_1 - 2s_4/\tan(\theta/2)\right)^2/24 \tag{D.10}$$

$$I_{yy} = \sigma_1 h_1^2/18 + +\sigma_1 \Delta h_1^2 - \sigma_2 h_2^2 - \sigma_2 \Delta h_2^2 \tag{D.11}$$

For triangular section where

$$\theta = s_1 \cos \frac{s_1}{2s_2} \tag{D.12}$$

$$h_1 = s_2 \sin \theta \tag{D.13}$$

$$h_2 = h_1 - s_4 \frac{1. + \cos\theta}{\cos\theta} \Delta h_1 = h_1 - h \tag{D.14}$$

$$\Delta h_2 = h_2 + s_4 - h \tag{D.15}$$

$$h = \frac{\sigma_1 h_1 - \sigma_2 (h_2 + s_4)}{\sigma_1 - \sigma_2} \tag{D.16}$$

In all the cases, the cross terms are zero and

$$I_{zz} = \frac{\Delta m \Delta l^2}{12} \tag{D.17}$$

where Δl is the length of each segment and $\Delta m = \rho\sigma\Delta l$ is the structural mass of the segment. If sufficient number of segments are used for each column, $I_{zz} = 0$ can be set for the segment.

The above moments of inertia are w.r.t. the principal axes fixed on the cross section of the column and have to be trasformed into those with respect to the global axes. If (X, Y, Z) are the axes that are through the centroid of the cross section and are parallel with the global axes, then the second moments of inertia of the solid cross sectional area about X, Y and Z axes are

$$I_{X_i X_j} = \rho \Delta l \sum_{k=1}^{3} \sum_{m=1}^{3} t_{ik} t_{jm} I_{x_k x_m} \tag{D.18}$$

where t_{ij} are the elements of the transformation matrix $[t]$

$$[t] = \begin{bmatrix} e_{x1} & e_{y1} & e_{z1} \\ e_{x2} & e_{y2} & e_{z2} \\ e_{x3} & e_{y3} & e_{z3} \end{bmatrix} \tag{D.19}$$

$$\vec{e}_x = \{e_{x1}, e_{x2}, e_{x3}\} \tag{D.20}$$

Denote $\vec{r}_k^c$ as the position vector of the centroid of k^{th} segment, i.e.

$$\vec{r}_k^c = \vec{r}_1 + \frac{(2k-1)\Delta l \vec{e}_z}{2} \tag{D.21}$$

for $k = 1, 2, ..., n$. The polar and second moments of inertia of the column with respect to a specified point $\vec{r}_p$ are given by

$$W_i = \Delta m \sum_{k=1}^{n} (\vec{r}_k^c - \vec{r}_p)_i \tag{D.22}$$

$$I^c_{X_i X_j} = n I_{X_i X_j} + \Delta m \sum_{k=1}^{n} (\vec{r}_k^c - \vec{r}_p)_i (\vec{r}_k^c - \vec{r}_p)_j \tag{D.23}$$

for $i, j = 1, 2, 3$.

APPENDIX E DRAG FORCE

For semi-submersible structures, which have a large displacement but relatively small water-plane area, the damping due to viscous drag force on the structure may become important relative to the radiation damping, especially at low frequencies.

Neglecting any lifting forces that may exist, the sectional drag force on any column member of the body is expressed as

$$F_j^v = \frac{1}{2} C_{dj} A_j ||\vec{V}|| V_j \tag{E.1}$$

where

F_v is the sectional drag force;

$j = 1, 2, 3$ indicates the three translational modes of motion;

C_{dj} is the drag coefficient;

A_j is a characteristic cross sectional dimension corresponding to the j^{th} mode of motion;

$\vec{V}$ is the total relative velocity normal to column axis; the relative velocity is between water particle velocity in waves, $\vec{U}_w$ and that of the moving column, $\dot{\vec{q}}_c$ taken at a reference point on the cross section; and

V_j is j^{th} component of $\vec{V}$;

$\vec{V}$ can be written as

$$\vec{V} = \vec{U}_w - \dot{\vec{q}}_c - (\vec{U}_w - \dot{\vec{q}}_c) \cdot \vec{t} \tag{E.2}$$

where $\vec{t}$ is the unit vector along the column axis. It is implied in the foregoing equations that the body cross-sectional dimension is small in comparison with the wave length so that the velocities of water particles do not change significantly within the cross section. This requirement is practically acceptable as the primary concern here is the viscous effect in the low frequency range.

Before the sectional force in equation (E.1) is integrated over the column length, it is linearized. The ways in which this is done are discussed by Chakrabarti[10]. Equation (E.1) becomes after linearization

$$F_j^v = \frac{4}{3\pi} C_{dJ} A_j ||\vec{U}_w||_n \left(\vec{U}_w - \dot{\vec{q}}_c\right)_{nj} \tag{E.3}$$

in which n indicates the direction normal to the column axis. The relative velocity amplitude is approximated by that of the wave motion under the assumption of small

amplitude motions of the body. Set $A_j = D$ with D being a characteristic dimension of the cross section. Assume that the body is composed of slender columns. If the axis of a column is in line with the translational motion of j^{th} mode, it does not induce any drag. The force in equation (E.3) is now integrated to arrive at the total force on the body

$$F_j^V = \int_{l_j} F_j^v dx_j \tag{E.4}$$

The moments of F_j^V are calculated acoordingly as

$$M_j^V = \int_{l_j} \left(\vec{r}_c \times \vec{F}^v\right)_j dx_j \tag{E.5}$$

It is noted that $\vec{F}^V$ and $\vec{M}^V$, when substituted into the equations of motion of the body, contribute a viscous damping term to the left-hand side and a drag force term to the right-hand side.

APPENDIX F THE FORCE COEFFICIENTS FOR AN ELASTIC SPRING

In the case of an external force exerted on the body by a simple massless linear elastic spring, let one end of the spring of unstretched length l_0 be fixed at point (x_1^0, x_2^0, x_3^0), and the other end be connected to the body at point (x_1, x_2, x_3). The point of connection on the body is denoted as $(\overline{x}_1, \overline{x}_2, \overline{x}_3)$ when the body is in its undisturbed position such that $\overline{r} - l_0 \geq 0$ where

$$\vec{\overline{r}} = (\overline{x}_1 - x_1^0)\vec{i}_1 + (\overline{x}_2 - x_2^0)\vec{i}_2 + (\overline{x}_3 - x_3^0)\vec{i}_3 \tag{F.1}$$

$$\overline{r}_j = \overline{r}\overline{e}_j \tag{F.2}$$

with i_j $j = 1, 2, 3$ being the unit vectors along the three coordinate axes respectively. Similarly, denote $\vec{r}$ as

$$\vec{r} = (x_1 - x_1^0)\vec{i}_1 + (x_2 - x_2^0)\vec{i}_2 + (x_3 - x_3^0)\vec{i}_3 \tag{F.3}$$

$$r_j = re_j \tag{F.4}$$

with

$$e_j = \frac{r_j}{r}$$

being the directional cosines of $\vec{r}$.

Let the spring force at an offset position of the body be $\vec{F}$ such that

$$\vec{F} = -F\vec{e} \tag{F.5}$$

$$F_j = -Fe_j = \overline{F}_j + \frac{\partial F_j}{\partial q_i}|_{\vec{r}=\vec{\overline{r}}} q_i \tag{F.6}$$

$$F = \begin{cases} k(r - l_0) & \text{if } r > l_0 \\ 0 & \text{if } r \leq l_0 \end{cases} \tag{F.7}$$

$$\frac{\partial F_j}{\partial q_i} = \frac{\partial F_j}{\partial r_k}\frac{\partial r_k}{\partial q_i}|_{\vec{r}=\vec{\overline{r}}} = T_{ji} \tag{F.8}$$

$$\vec{r} = \sum_{j=1}^{3}(\overline{x}_j + dr_j - x_j^0)\vec{i}_j \tag{F.9}$$

$$\vec{dr} = \vec{q} + \vec{\alpha} \times (\vec{\overline{r}} - \vec{r}_0) \tag{F.10}$$

$$\frac{\partial F_j}{\partial r_k} = [T_{jk}^1] = -\frac{k}{\overline{r}^2}(\overline{e}_k l_0 \overline{r}_j + (\overline{r} - l_0)\overline{r}\delta_{jk}) \tag{F.11}$$

$$\frac{\partial r_k}{\partial q_i}|_{\vec{r}=\vec{\overline{r}}} = [T^2_{ki}] = \begin{bmatrix} 1 & 0 & 0 & 0 & X_3 & -X_2 \\ 0 & 1 & 0 & -X_3 & 0 & X_1 \\ 0 & 0 & 1 & X_2 & -X_1 & 0 \end{bmatrix} \tag{F.12}$$

so that $[T] = [T^1][T^2]$. $X_i = \overline{x}_i - x_{0i}$. $\overline{F}_j$ for $j = 1, 2, 3$ correspond to the static components, namely, the pretension.

The above simple spring model is frequently used to represent the restraining forces of mooring lines attached to the floating body. The mooring lines are often of catenary type and their characteristics are known to be nonlinear in terms of the end displacement. Nonetheless, the above simplification is usually justified under the assumption of small amplitude motions of the floating body.

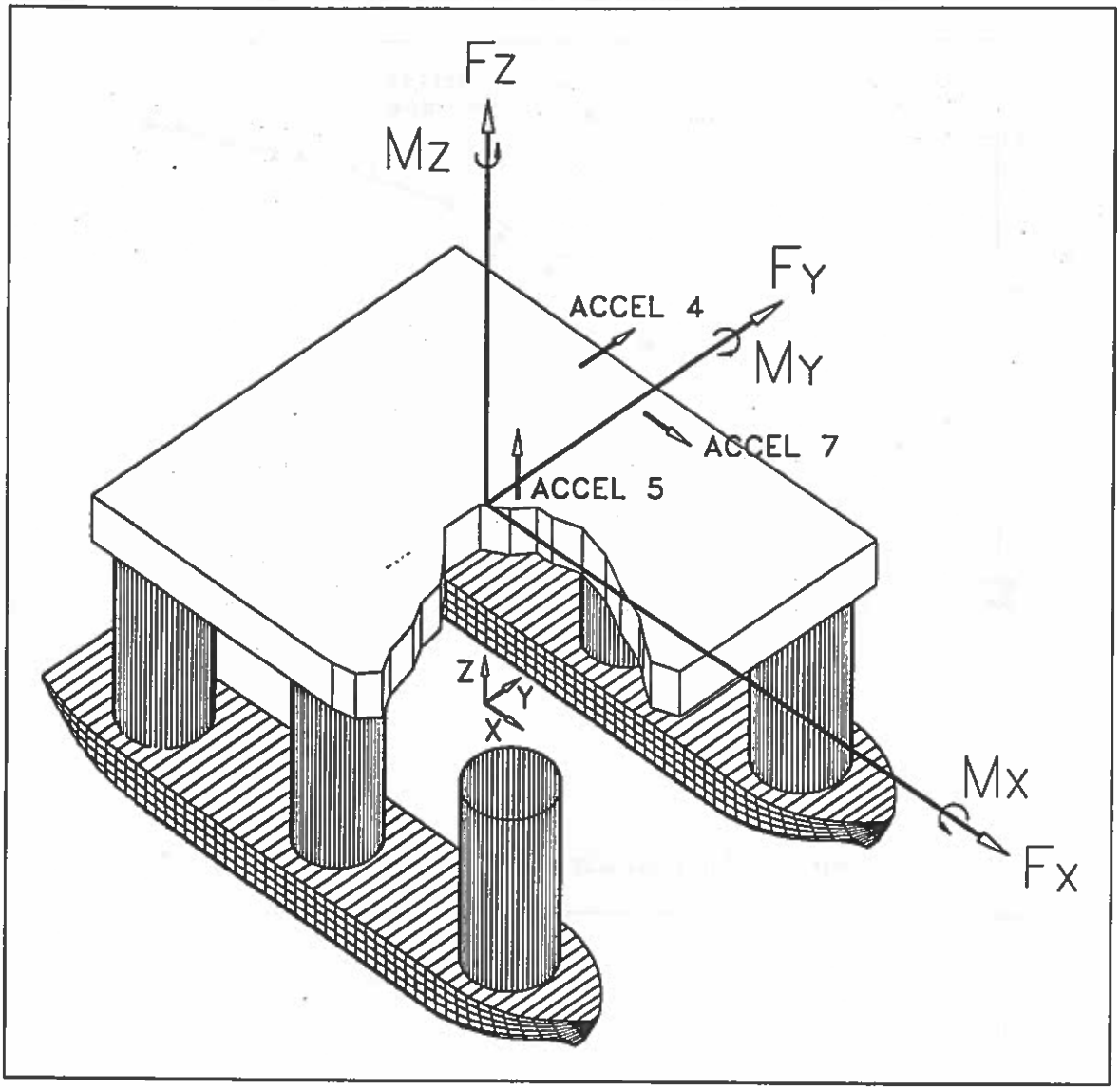

Figure 2 A sketch of the model of the Glomar Arctic III semi-submersible.

Figure 3 Measured and numerically predicted sway RAO at body CG in beam seas.

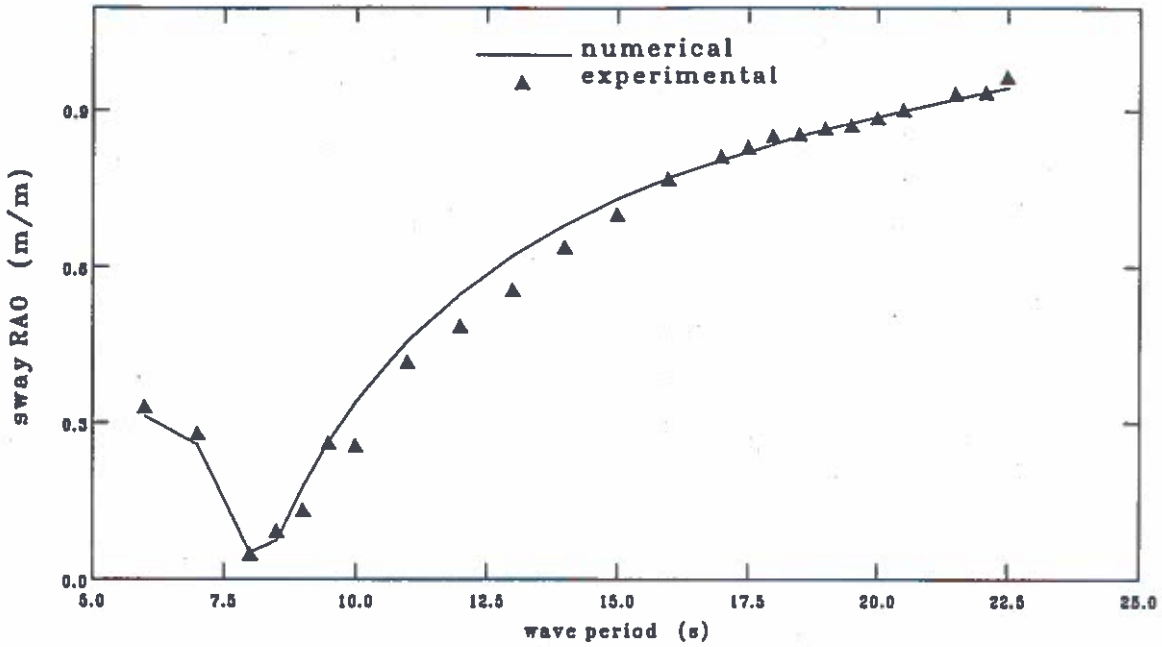

Figure 4 Measured and numerically predicted heave RAO at body CG in beam seas.

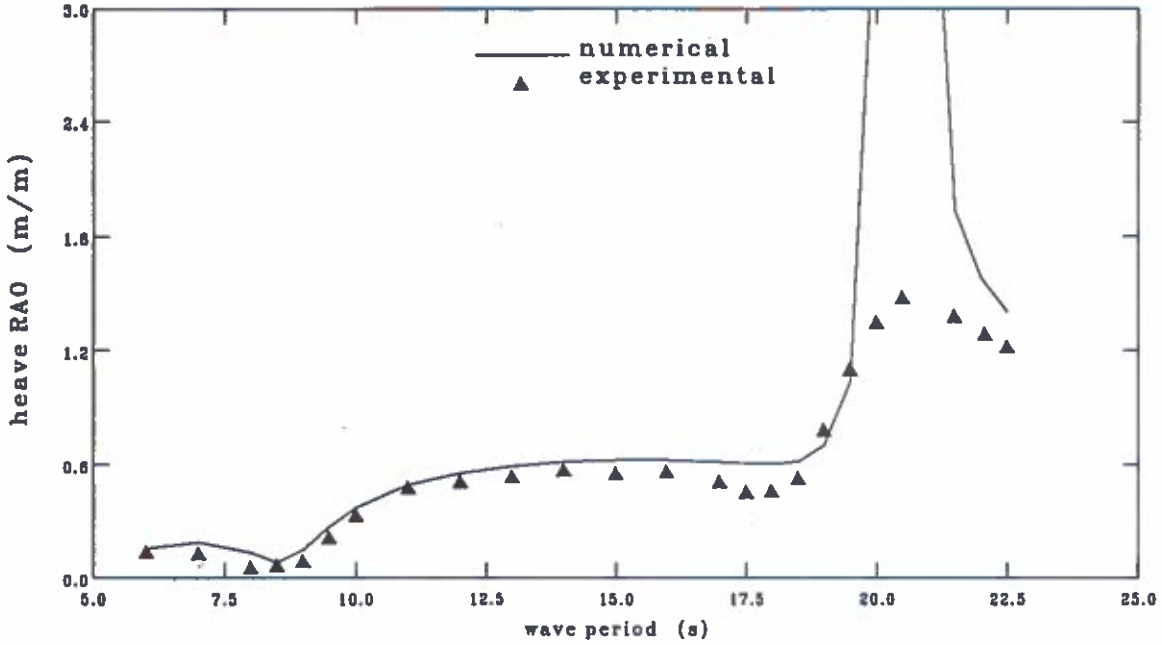

Figure 5 Measured and numerically predicted roll RAO in beam seas.

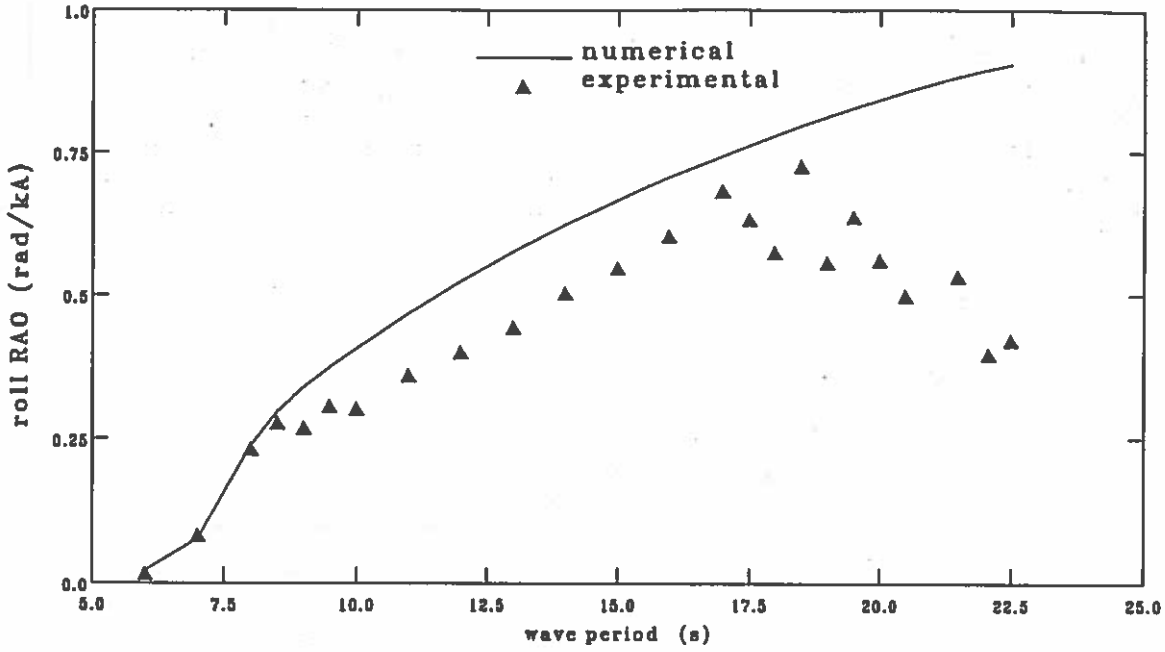

Figure 6 Measured and numerically predicted internal sway force ($F_{uy}^{(1)}$) RAO in beam seas.

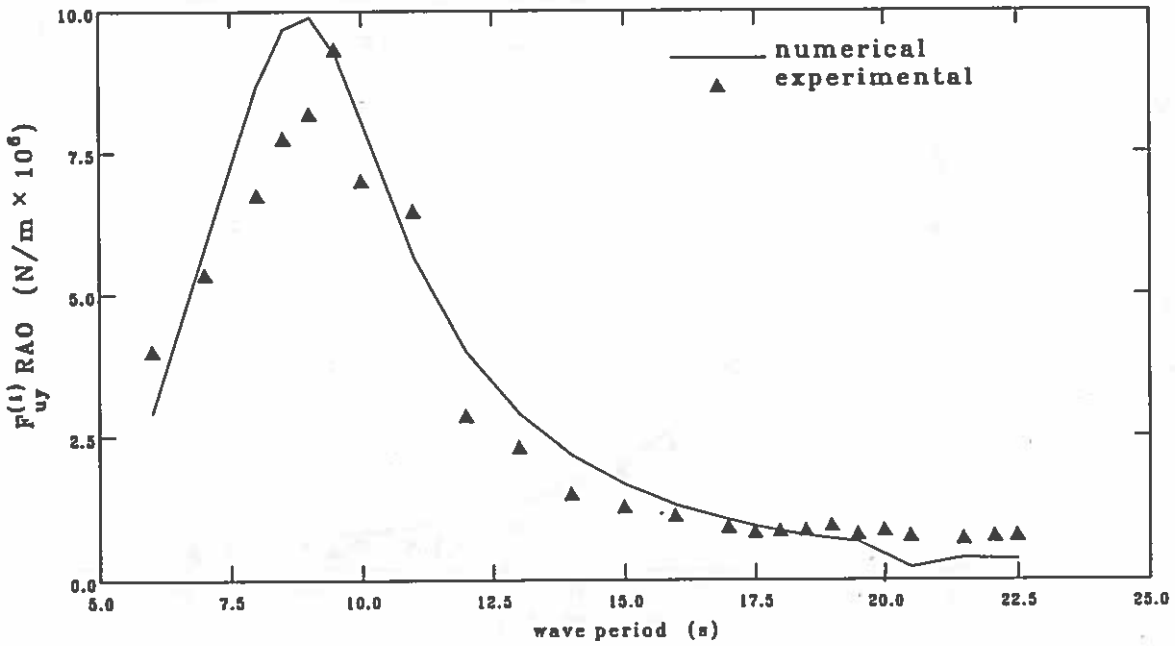

Figure 7 Measured and numerically predicted internal heave force ($F_{uz}^{(1)}$) RAO in beam seas.

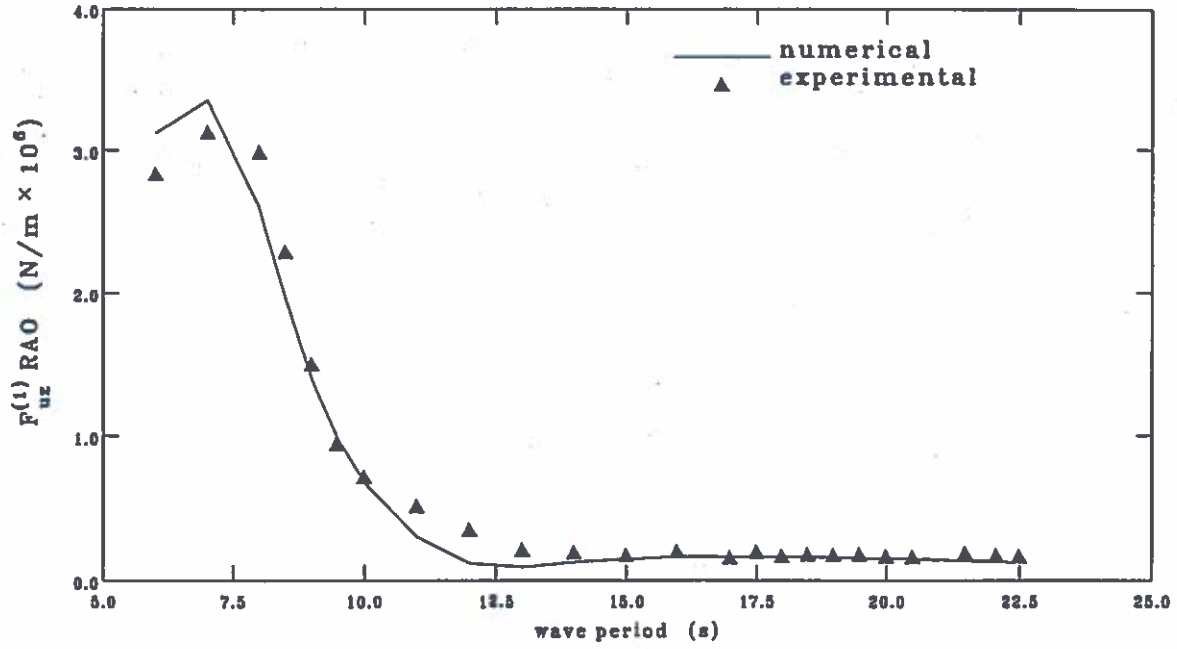

Figure 8 Measured and numerically predicted internal roll moment ($M_{ux}^{(1)}$) RAO in beam seas.